Journal of Dental Sciences xxx (xxxx) xxx

Available online at www.sciencedirect.com

ScienceDirect

journal homepage: www.e-jds.com

Correspondence

Enhancing cone-beam computed tomography detail and interpretation with a generative adversarial network-driven artificial intelligence framework

KEYWORDS
Cone-beam computed tomography;
Generative adversarial network;
Image translation;
Dental imaging;
Structural consistency

Cone-beam computed tomography (CBCT) now plays an essential role in daily dental practice, providing three-dimensional views that clinicians rely on for implant planning, endodontic treatment decisions, orthodontic assessments, and the evaluation of maxillofacial conditions.[1] However, the clarity and diagnostic usefulness of CBCT images can vary considerably in real clinical settings. Factors such as voxel size, field of view (FOV), and specific acquisition parameters influence how well subtle anatomic details are displayed. In addition, motion during scanning, scatter from metallic restorations, and limitations imposed by a restricted FOV may further reduce the visibility of fine or peripheral structures. These issues often result in images that are adequate for general assessment but less reliable when precise boundary interpretation is required.

In our previous study,[2] we developed an AI-based strategy to analyze CBCT scans by combining semantic segmentation with computer vision tools. Through that work, it became apparent that CBCT—despite its usefulness in capturing volumetric information—often fails to display crisp internal boundaries within teeth. The blurred transitions between structures made it difficult to interpret fine anatomical details, particularly in regions where subtle changes matter clinically. While histopathology continues to serve as the definitive reference for tissue evaluation, it remains invasive, labor-intensive, and impossible to obtain repeatedly from living patients.[3] To narrow the gap between what clinicians can visualize in vivo and the level of detail provided by microscopic examination, we developed a cycle-consistent generative adversarial network (CycleGAN). This model was designed to generate histology-like images directly from standard CBCT slices, offering a non-invasive way to approximate tissue-level information without the need for biopsy.[4]

In this preliminary work, we used a CycleGAN to carry out two-way translation between the imaging domains under study. After generating the cross-domain images, each output was cycled back to its original form to examine how well the underlying structures were preserved. For evaluation, five test samples were assessed using two widely adopted image-quality measures: the structural similarity index (SSIM) and the peak signal-to-noise ratio (PSNR).[5] The model also incorporated a cycle-consistency component to help maintain anatomical coherence during translation. Lower cycle-loss values reflected reconstructions that more closely resembled the original

https://doi.org/10.1016/j.jds.2025.12.001

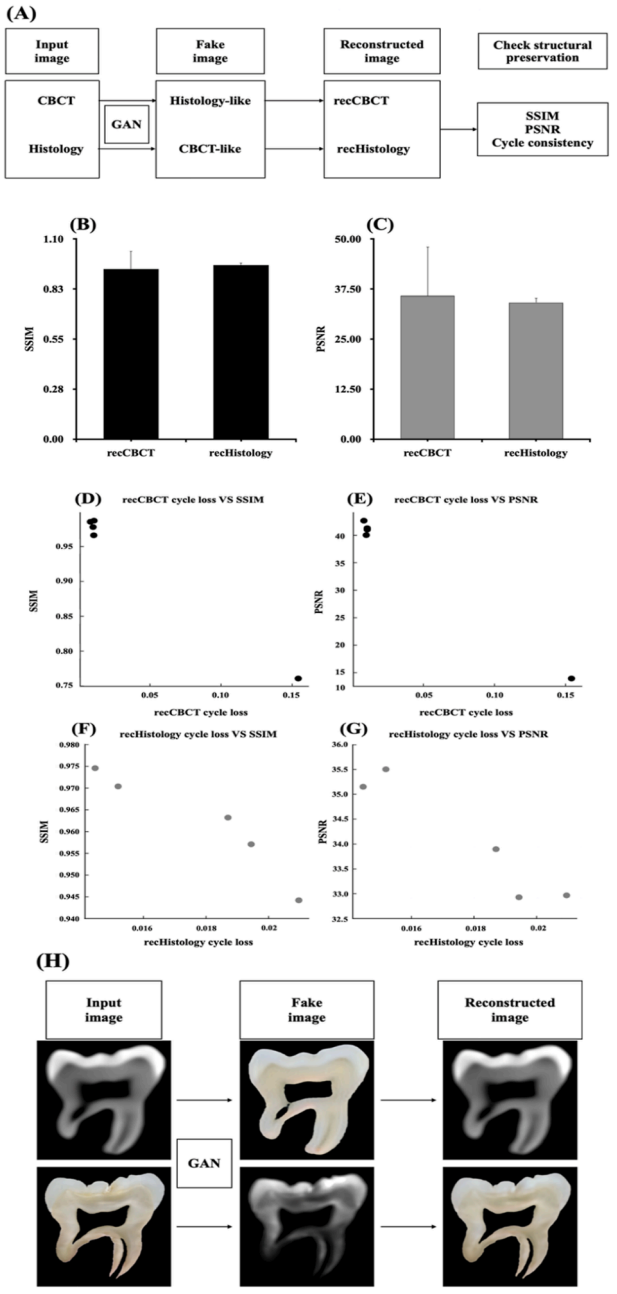

Figure 1 A process for enhancing the cone-beam computed tomography (CBCT) image sharpness through the generative adversarial network (GAN)-driven methods. (A) Overview of the image-translation workflow. CBCT and histology images were each processed through a cycle-consistent GAN (CycleGAN) model to generate cross-domain synthetic images (Histology-like or CBCT-like images). The synthesized images were then translated back to their original domains to obtain the reconstructed outputs (recCBCT and recHistology images). These reconstructions were inspected for the preservation of key anatomical structures, followed by quantitative evaluation using the structural similarity index (SSIM) and the peak signal-to-noise ratio (PSNR), and cycle-consistency loss. (B and C) Mean SSIM and PSNR values for reconstructed CBCT and histology images. Error bars indicate standard deviations across all samples. (D and E) These panels illustrate how the cycle-consistency loss of recCBCT changes in relation to its SSIM and PSNR values. Data points shown in black indicate measurements from the CBCT reconstructions. (F and G) Similar plots are presented for the histology pathway, demonstrating how recHistology cycle-loss corresponds with its SSIM and PSNR. Gray markers denote results from the histology group. (H) Representative qualitative examples of the translation-reconstruction process. Each panel displays the original input image, its cross-domain synthesized output, and the final reconstructed image after completing the full cycle. Both CBCT and histology pathways demonstrate the preservation of the major morphological characteristics—supporting the reliability of the model in maintaining structural information during the domain translation.

images, indicating fewer distortions introduced by the translation process (Fig. 1A).

Across the samples we assessed, the reconstructed CBCT images (recCBCT) showed a high degree of similarity to their corresponding originals, with a mean SSIM of 0.94 ± 0.10. The reconstructed histology images (recHistology) demonstrated a comparable level of consistency, reaching an average SSIM of 0.96 ± 0.01 when compared with the reference histologic sections (Fig. 1B). In addition, the PSNR measurements supported the overall quality of both reconstruction pathways. The recCBCT images produced an average PSNR of 35.78 ± 12.24 dB, while the recHistology group reached 34.09 ± 1.20 dB, indicating that both sets maintained strong signal integrity relative to their ground truth counterparts (Fig. 1C).

Within the CBCT translation pathway, higher recCBCT cycle-loss values were closely associated with lower SSIM and PSNR scores ($r = -0.997$ and $r = -0.998$, respectively) (Fig. 1D and E). The strength of these correlations, which approached -1, suggests that even modest increases in cycle loss were accompanied by a clear drop in structural similarity and overall signal quality. In the histology translation pathway, a comparable pattern was noted. Although the correlations were slightly weaker than those seen in the CBCT direction, the recHistology cycle-loss values still showed a strong negative relationship with both SSIM ($r = -0.948$) and PSNR ($r = -0.954$) (Fig. 1F and G). Cases with lower cycle loss tended to retain clearer structural definition, whereas higher-loss samples consistently displayed reduced alignment with their corresponding reference images. Taken together, these observations indicate that cycle-consistency loss serves as a useful indicator of how well the network maintains structural detail throughout the translation process.

A representative example of the model's behavior is illustrated in Fig. 1H. When a CBCT slice served as the input, the CycleGAN generated a histology-like image that preserved the overall tooth outline and major internal features, while adding textures similar to those seen in real tissue sections. Cycling the image back to the CBCT domain produced a reconstruction that remained closely aligned with the original scan, indicating that the core structural elements were largely maintained throughout the process (upper panel of Fig. 1H). A comparable pattern was observed when translating in the opposite direction: starting with a histology image, our network generated a CBCT-like representation that successfully captured the

broad radiographic characteristics. The subsequent reconstruction process continued to reflect the essential details of the source specimen. While these synthesized images were not intended to serve as a substitute for true microscopic examination, this example clearly illustrated the model's capacity to produce coherent cross-domain translations in both directions while preserving recognizable anatomical information (bottom panel of Fig. 1H).

Although this proof-of-concept study offered promising insights, several inherent limitations warrant careful consideration. The number of cases included was modest, and the range of available histologic specimens was fairly limited. Furthermore, acquiring true one-to-one, perfectly aligned CBCT—histology pairs remains a significant challenge in routine clinical practice, which inherently complicates the process of building a fully aligned and robust training dataset. Therefore, the strong link we identified between general image quality and cycle loss indicates that these measures could serve as useful guides when fine-tuning future iterations of this model. Broader datasets, improved image registration methods, and specific adjustments tailored to individual dental tissue types may further strengthen the system's consistency and clinical utility. Overall, our results suggest that the cycle-consistent GAN framework can support bidirectional translation between the imaging domains, enabling one modality to be inferred or generated from the other without the need for any invasive procedures.

Declaration of competing interest

The authors have no conflicts of interest relevant to this article.

Acknowledgments

This research was funded by a general grant from the National Science and Technology Council, Taiwan (NSTC 114-2314-B-038-051) to Wei-Chun Lin.

References

1. Baccher S, Gowdar IM, Guruprasad Y, et al. CBCT: a comprehensive overview of its applications and clinical significance in dentistry. *J Pharm BioAllied Sci* 2024;16:1923—5.
2. Lin YC, Cheng FC, Lin WC, Chiang CP. Artificial intelligence measurement of multi-layer tooth structures using semantic segmentation and computer vision. *J Dent Sci* 2025;20:723—5.
3. Gliga A, Imre M, Grandini S, et al. The limitations of periapical x-ray assessment in endodontic diagnosis-a systematic review. *J Clin Med* 2023;12:4647.
4. Chen P, Shen B, Yang Y, et al. Deep learning super-resolution for dental CBCT using micro-CT reference and edge loss function. *J Dent* 2025;164:106209.
5. Wang Z, Bovik AC, Sheikh HR, Simoncelli EP. Image quality assessment: from error visibility to structural similarity. *IEEE Trans Image Process* 2004;13:600—12.

Chi-Yu Lin
School of Dental Technology, College of Oral Medicine, Taipei Medical University, Taipei, Taiwan

Che-Ming Liu
School of Dentistry, College of Oral Medicine, Taipei Medical University, Taipei, Taiwan
Department of Dentistry, Wan Fang Hospital, Taipei Medical University, Taipei, Taiwan

Yu-Chieh Lin
Digital Medicine Center, Translational Health Research Institute, Vilnius University, Vilnius, Lithuania
Institute of Research, Development and Innovation, IMU University, Kuala Lumpur, Malaysia

Wei-Chun Lin*
School of Dental Technology, College of Oral Medicine, Taipei Medical University, Taipei, Taiwan
Department of Dentistry, Wan Fang Hospital, Taipei Medical University, Taipei, Taiwan

* Corresponding author. School of Dental Technology, College of Oral Medicine, Taipei Medical University, No. 250, Wu-Xing Street, Taipei, 11031, Taiwan.
E-mail address: weichun1253@tmu.edu.tw (W.-C. Lin)

Received 29 November 2025
Final revision received 30 November 2025
Available online ■ ■ ■